Fluid Phase Equilibria 375 (2014) 80–88

Contents lists available at ScienceDirect

Fluid Phase Equilibria

journal homepage: www.elsevier.com/locate/fluid

The effect of the cation aromaticity upon the thermophysical properties of piperidinium- and pyridinium-based ionic liquids

Arijit Bhattacharjee, Pedro J. Carvalho*, João A.P. Coutinho

CICECO, Departamento de Química, Universidade de Aveiro, 3810-193 Aveiro, Portugal

ARTICLE INFO

Article history:
Received 2 March 2014
Received in revised form 23 April 2014
Accepted 26 April 2014
Available online 4 May 2014

Keywords:
Ionic liquids
Density
Viscosity
Surface tension
Refractive index

ABSTRACT

Experimental data on density, viscosity, refractive index and surface tension of four ILs: 1-Methyl-1-propylpiperidinium bis(trifluoromethylsulfonyl)imide [C_3C_1Pip][NTf_2], 1-Butyl-1-methylpiperidinium bis(trifluoromethylsulfonyl)imide [C_4C_1Pip][NTf_2], 3-Methyl-1-propylpyridinium bis(trifluoromethylsulfonyl)imide [C_3C_1Py][NTf_2] and 1-Butyl-3-methylpyridinium bis(trifluoromethylsulfonyl)imide [C_4C_1Py][NTf_2] were measured in the temperature range between 288.15 and 353.15 K and at atmospheric pressure to evaluate the impact of the cation's aromaticity upon the thermophysical properties of ionic liquids. The properties investigated show that the pyridinium aromatic ring, with its π–π interactions, leads to a more rigid, compact and organized liquid phase, while the less rigid structure of the piperidinium cation induces more entanglement and consequently higher resistance to shear stress (higher viscosities) and better surface arrangement (higher surface tensions). The group contribution methods proposed by Gardas and Coutinho were also evaluated and fitted to the experimental data, allowing the proposal of new parameters for the cations investigated.

1. Introduction

During the past decade, through sustained research, Ionic liquids (ILs) became valid replacements for many volatile organic compounds (VOCs) used in industry. ILs are organic salts, thus ionic compounds, that are liquid at temperatures below 100 °C due to the asymmetry and charge dispersion of their organic and inorganic ions. They are receiving increasing attention due to their unique thermophysical properties such as negligible vapor pressure at room temperature [1], relatively high thermal stability and large liquidus temperature range [2], non-flammability [3], high ionic conductivity and the possibility of preparing them to meet specific needs that lead to the designation of '*designer solvents*'. These properties result from not only the large number of possible combinations of cations and anions, allowing thus the tuning of their properties for specific applications [4–6], but also from a further fine tuning that can be achieved by playing with the structure of their ions, optimizing yield, selectivity, substrate solubility, product separation, and even enantioselectivity [1,7–10].

The design of industrial processes and new products based on ILs requires accurate and adequately characterized thermophysical data such as viscosity, density, and interfacial tension. These data are needed for the development of models for process design, energy efficiency, control of chemical processes, and in the evaluation of their potential environmental impact. Furthermore, the study of these properties can provide information not only about the IL structure but also yield qualitative insights concerning their interactions at a molecular level.

The most studied ILs are those based on the imidazolium cation [11–22]. Fewer studies have been devoted to the viscosities and densities of pyridinium- [18,23–33] and piperidinium-based ILs [18,29,34,35]. As for the anion, bis(trifluoromethylsulfonyl)imide is one of the most interesting anions as far as water stability [36], high thermal stability, enhanced hydrophobicity [37] and relatively low viscosity are concerned.

In this work, density, viscosity, refractive index and surface tension data of four ILs with the bis(trifluoromethylsulfonyl)imide anion were measured in the temperature range between 288.15 and 353.15 K and at atmospheric pressure. The objective of this work is to investigate the relation between the measured properties and the ionic structures and ultimately establishing principles for the molecular design of ILs. For that purpose, the [NTf_2] anion was studied in combination with four cations, namely 1-Methyl-1-propylpiperidinium bis(trifluoromethylsulfonyl)imide

* Corresponding author. Tel.: +351 234 370 958; fax: +351 234 370 084.
E-mail address: quijorge@ua.pt (P.J. Carvalho).

http://dx.doi.org/10.1016/j.fluid.2014.04.029
0378-3812/

Table 1
Ionic structures, names, molecular weight and water content of the studied ILs.

ILs	Ionic structure
1-Methyl-1-propylpiperidinium bis(trifluoromethylsulfonyl)imide **[C_3C_1Pip][NTf_2]** (422.41 g mol^{-1}; wt% = 0.1420)	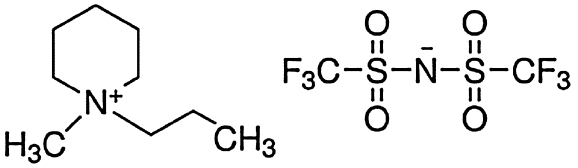
1-Butyl-1-methylpiperidinium bis(trifluoromethylsulfonyl)imide **[C_4C_1Pip][NTf_2]** (436.44 g mol^{-1}; wt% = 0.1007)	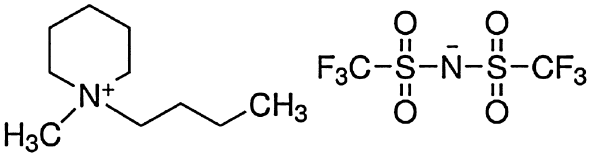
3-Methyl-1-propylpyridinium bis(trifluoromethylsulfonyl)imide **[C_3C_1Py][NTf_2]** (416.36 g mol^{-1}; wt% = 0.0704)	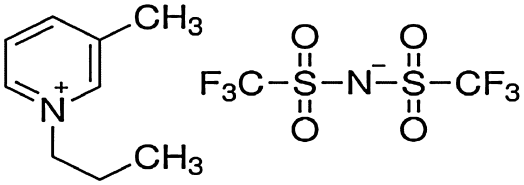
1-Butyl-3-methylpyridinium bis(trifluoromethylsulfonyl)imide **[C_4C_1Py][NTf_2]** (430.39 g mol^{-1}; wt% = 0.0615)	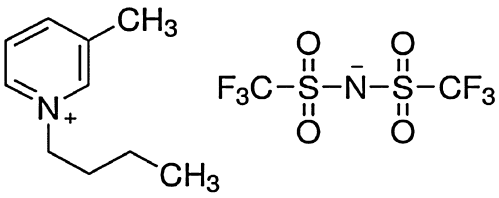

[C_3C_1Pip], 1-Butyl-1-methylpiperidinium bis(trifluoromethylsulfonyl)imide [C_4C_1Pip], 3-Methyl-1-propylpyridinium bis(trifluoromethylsulfonyl)imide [C_3C_1Py], 1-Butyl-3-methylpyridinium bis(trifluoromethylsulfonyl)imide [C_4C_1Py] in order to investigate the effect of the cation aromaticity on the piperidinium and pyridinium cation-based ILs thermophysical properties.

The Gardas and Coutinho [38,39] group contribution methods were applied to the description of the pure component densities, viscosities and refractive indices and new group contribution parameters were estimated whenever needed.

2. Materials and methods

2.1. Materials

Four ionic liquids were here studied namely 1-Methyl-1-propylpiperidinium bis(trifluoromethylsulfonyl)imide [C_3C_1Pip][NTf_2], 3-Methyl-1-propylpyridinium bis(trifluoromethylsulfonyl)imide [C_3C_1Py][NTf_2], 1-Butyl-1-methylpiperidinium bis(trifluoromethylsulfonyl)imide [C_4C_1Pip][NTf_2] and 1-Butyl-3-methylpyridinium bis(trifluoromethylsulfonyl)imide [C_4C_1Py][NTf_2]. The ionic structures of these ILs are presented in Table 1. The ionic liquids were acquired from IoLiTec with mass fraction purities higher than 99%. The water content plays an important role in the IL properties, such as surface tension and viscosity [14,40,41] thus to remove traces of water and volatile compounds from the ILs, individual samples of each fluid were dried at moderate temperature (≈313 K), high vacuum (≈10^{-1} Pa) and stirring for a minimum period of at least 48 h prior to the measurements. The purity of each IL was checked by ^{1}H NMR, ^{19}F NMR and ^{13}C NMR, before and after the measurement procedure, in order to confirm that no degradation, due to temperature and contact with water, occurred during the measurements. The final IL water content was determined with a Metrohm 831 Karl Fischer coulometer (using the Hydranal - Coulomat AG from Riedel-de Haën as analyte). The average water content and the molecular weight of each IL are presented in Table 1.

2.2. Experimental

2.2.1. Density and viscosity

Density (ρ) and dynamic viscosity (η) measurements were carried out using an automated SVM 3000 Anton Paar rotational Stabinger viscometer-densimeter in the temperature range from 283.15 to 353.15 K and at atmospheric pressure. The absolute uncertainty in density is ±0.5 kg m^{-3} and the relative uncertainty in dynamic viscosity is ±0.35%. The relative uncertainty in temperature is within ±0.02 K. Further details about the use of the equipment and method for determination of densities and viscosities can be found elsewhere [14,42].

2.2.2. Refractive index

Measurements of refractive index (n_D) were performed at 589.3 nm using an automated Abbemat 500 Anton Paar refractometer, able to measure both liquid and solid samples. Refractive index measurements were carried out in the temperature range from 288.15 to 353.15 K and at atmospheric pressure. The Abbemat 500 Anton Paar refractometer uses reflected light to measure the refractive index, where the sample on the top of the measuring prism is irradiated from different angles by a light-emitting diode (LED). The measurements were carried out under a dry atmosphere by means of a close chamber filled with silica gel. At least four measurements were taken for each sample at each temperature to ensure the effectiveness of the measurements.

The maximum deviation in temperature is ±0.01 K, and the maximum uncertainty in the refractive index measurements is ±2 × 10^{-5} n_D. Previous data for other ILs are published elsewhere

and support the viability of the equipment to determine accurate refractive indices of IL samples [13,43].

2.2.3. Surface tension

The surface tension of each compound was determined through the analysis of the shape of the pendant drop using a Dataphysics contact angle system OCA-20. Drop volumes of $10 \pm 2\,\mu L$, depending on the IL, were obtained using a Hamilton DS 500/GT syringe with a Teflon coated needle. The needle was placed in a double-jacketed aluminum air chamber capable of maintaining the temperature within ±0.1 K. The temperature was attained by circulating water in the double jacketed aluminium cell by means of a Julabo F-25 water bath. The temperature inside the aluminium chamber was measured with a Pt100 within ±0.1 K which is placed at a distance of approximately 2 cm of the liquid drop. The surface tension measurements were performed in the temperature range from 293.15 to 344.15 K and at atmospheric pressure. After reaching a specific temperature, the measurements were carried out after 30 min to guarantee the thermal equilibrium. Silica gel was kept inside the air chamber to avoid the adsorption of moisture. For the surface tension determination, at each temperature and for each IL, at least three drops were formed and analyzed. For each drop, an average of 100 images was additionally captured. The analysis of the drop shape was performed with the software modules SCA 20. The density data used for the ILs were those determined in this work. The equipment was previously validated through the measurement of the surface tension of ultra-pure water, decane and dodecane and shown to be accurate to measure ILs [44].

3. Results and discussions

3.1. Density

The density measurements for the four ILs were carried out in the temperature range of 288.15–353.15 K at atmospheric pressure and are reported in Table 2 and depicted in Fig. 1. The density of the ILs proved to be dependent on the IL cation's alkyl chain length and, to a lower extent, on the temperature (in the evaluated temperature range). Similar to what was observed for other cations families [18,19,30,45–48], the densities decrease with temperature and with the increase of the cation alkyl chain length, as shown in Fig. 1. Furthermore, the density is greatly affected by the aromaticity of the IL, with the double bonds of the aromatic pyridinium ring leading to lower cation volumes ([C_3C_1Pip]: 1418.66 nm^3; [C_3C_1Py]: 1317.24 nm^3; [C_4C_1Pip]: 1567.52 nm^3; [C_4C_1Py]: 1465.00 nm^3) as obtained by COSMO-RS [49,50] and therefore, higher densities than those of the piperidinium. The difference of the cation volumes, between the pyridinium and piperidinium, lead to differences on the density similar to that observed for the addition of a methyl group in the cation alkyl chain.

Molar volumes, V_m, were calculated as:

$$V_m = \frac{M}{\rho} \quad (1)$$

where M and ρ are the molar mass and the density of the studied IL, respectively, and are reported in Table 2 as function of temperature. An average molar volume change of 16.8 cm^3 mol^{-1} is observed by the addition of a –CH_2 group to the piperidinum and pyridinium cations. These –CH_2 molar volume increment is in good agreement with that reported previously by us [18,19,45] and other authors [7,16,17,51,52] for imidazolium based ILs. This observation corroborates the well-established notion that the density of ILs is an additive property with ion-independent [46] molar volume increments of 17.1 cm^3 mol^{-1}, at 298.15 K, per each –CH_2 group [7,16–19,51,52].

Table 2
Densities, ρ (kg m^{-3}), molar volumes, V_m (m^3 mol^{-1}), viscosities, η (mPa s) and refractive index values, n_D, of the studied ILs as function of temperature and at atmospheric pressure.

	[C_3C_1Pip][NTf_2]				[C_4C_1Pip][NTf_2]				[C_3C_1Py][NTf_2]				[C_4C_1Py][NTf_2]			
T (K)	ρ	10^6V_m	η	n_D	ρ	10^6V_m	η	n_D	ρ	10^6V_m	η	n_D	ρ	10^6V_m	η	n_D
288.15	1420.3	297.41	274.0	1.43004	1389.7	314.05	344.9	1.43208	1458.4	285.49	88.9	1.44734	1424.2	302.20	107.8	1.44845
293.15	1415.8	298.35	198.1	1.42865	1385.2	315.07	247.7	1.43066	1453.6	286.43	68.7	1.44581	1419.6	303.18	82.7	1.44694
298.15	1411.4	299.28	145.6	1.42739	1380.8	316.08	180.2	1.42928	1448.8	287.38	54.3	1.44440	1414.9	304.18	64.7	1.44566
303.15	1407.0	300.22	110.4	1.42586	1376.5	317.07	135.4	1.42784	1444.1	288.32	43.7	1.44279	1410.3	305.18	51.7	1.44397
308.15	1402.6	301.16	85.6	1.42444	1372.2	318.06	104.0	1.42646	1439.3	289.28	35.7	1.44129	1405.7	306.17	42.0	1.44249
313.15	1398.2	302.11	67.9	1.42304	1367.9	319.06	81.7	1.42505	1434.6	290.23	29.6	1.43983	1401.1	307.18	34.6	1.44103
318.15	1393.9	303.04	54.4	1.42165	1363.6	320.06	64.9	1.42366	1430.0	291.16	25.0	1.43836	1396.6	308.17	28.9	1.43955
323.15	1389.6	303.98	44.5	1.42027	1359.4	321.05	52.5	1.42231	1425.3	292.12	21.2	1.43693	1392.1	309.17	24.4	1.43810
328.15	1385.3	304.92	36.9	1.41894	1355.2	322.05	43.2	1.42091	1420.7	293.07	18.3	1.43546	1387.6	310.17	20.8	1.43668
333.15	1381.0	305.87	31.0	1.41758	1351.0	323.05	36.0	1.41957	1416.1	294.02	15.9	1.43405	1383.1	311.18	17.9	1.43524
338.15	1376.7	306.83	26.2	1.41624	1346.8	324.06	30.2	1.41825	1411.5	294.98	13.9	1.43266	1378.7	312.17	15.5	1.43382
343.15	1372.5	307.77	22.5	1.41489	1342.7	325.05	25.7	1.41690	1407.0	295.92	12.2	1.43120	1374.3	313.17	13.6	1.43240
348.15	1368.3	308.71	19.5	1.41357	1338.6	326.04	22.1	1.41558	1402.5	296.87	10.9	1.42977	1369.9	314.18	12.0	1.43097
353.15	1364.1	309.66	17.0	1.41227	1334.5	327.04	19.2	1.41423	1398.0	297.83	9.7	1.42839	1365.5	315.19	10.7	1.42953

[a] Standard temperature uncertainty is $u(T) = \pm 0.02$ K and the combined expanded uncertainties, U_c, are $U_c(\rho) = \pm 0.5$ kg m^{-3}; $U_c(\eta) = 0.35\%$; $U_c(n_D) = 2 \times 10^{-5}$ with a 95% confidence level.

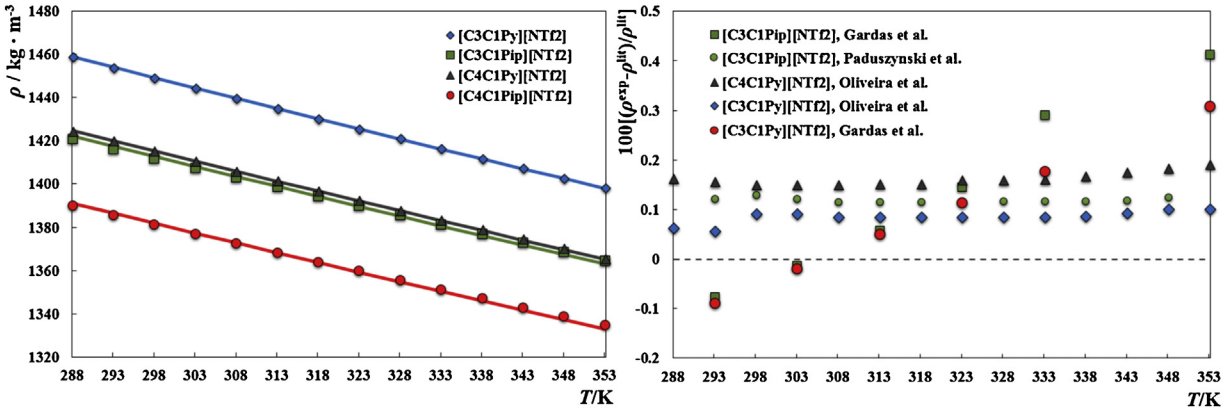

Fig. 1. Density as function of temperature (left) and average relative deviations between this work experimental data and those available in the literature [18,30,35,53]. The solid lines represent the Gardas and Coutinho [39] contribution method.

Density data for some of the studied ILs is available in the literature [18,30]. The relative deviations between the density data measured on this work and that available in the literature [18,30] are displayed in Fig. 1. To the best of our knowledge, no literature data, on densities, is available for $[C_4C_1Pip][NTf_2]$. Experimental data for $[C_3C_1Pip][NTf_2]$, $[C_3C_1Py][NTf_2]$, and $[C_4C_1Py][NTf_2]$ are in good agreement with the available literature values, with absolute relative average deviations ranging from 0.08% to 2% [18,30,35,53]. The absolute relative average deviations towards the $[C_3C_1Pip][NTf_2]$ previously measured by us [18] and Paduszynski et al. [53] are 0.17% and 0.12%, respectively. Liu et al. [35] reported the density of $[C_3C_1Pip][NTf_2]$ at 298.15 K with deviations of 2%. These deviations could be related to the experimental technique employed by the authors. They determined the IL density using a pycnometer (through weighting three 1.0 mL samples) at room temperature; a technique that, inherently, carries large uncertainties. Both $[C_3C_1Py][NTf_2]$ and $[C_4C_1Py][NTf_2]$ were previously investigated by us [18,30] and absolute average relative deviations within 0.16%, for the later, and 0.08% and 0.13%, for the first were obtained here. These deviations, although small may be related essentially to the variance of trace impurities, intrinsic to different production lots, and/or small variations on the ILs water content.

The molar volumes of the studied ILs, increase with the effective cation size in the order: $[C_3C_1Py]^+ < [C_3C_1Pip]^+ < [C_4C_1Py]^+ < [C_4C_1Pip]^+$. If one takes into account also the results for an aromatic imidazolium, $[C_4C_1im][NTf_2]$ [51], and an non-aromatic pyrrolidinium, $[C_4C_1Pyr][NTf_2]$ [18], the molar volumes increase with the IL molecular weight, while the density values present the opposite behavior: $[C_4C_1Pip]^+ < [C_4C_1Pyr]^+ < [C_4C_1Py]^+ < [C_4C_1im]^+$. This behavior seems, once more, related to the effect of the aromaticity of the cation on the density, with the aromatic ring double bonds leading to smaller cations and therefore, higher densities.

Gardas and Coutinho [39] extended the Ye and Shreeve [54] approach to the estimation of ionic liquid densities for a wide range of temperature, 288.15–353.15 K, pressures, 0.10–100 MPa, and ILs families according to the equation

$$\rho = \frac{M}{NV(a + bT + cp)} \quad (2)$$

where ρ is the density in kg m^{-3}; M the molecular weight in kg mol^{-1}; N the Avogadro constant; V the molecular volume in Å^3, T the temperature in K and p the pressure in MPa. The universal coefficients a, b and c are 0.8005 ± 0.0002, $6.652 \times 10^{-4} \pm 0.007 \times 10^{-4}$ K^{-1} and $-5.919 \times 10^{-4} \pm 0.024 \times 10^{-4}$ MPa^{-1}, respectively, at 95% confidence level. Molecular volumes for the new cations were fitted to the measured density data and the densities obtained are in good agreement with data, as shown in Fig. 1, with an absolute relative average deviation of 0.056%, 0.059%, 0.0092% and 0.015% for the $[C_3C_1Pip][NTf_2]$, $[C_4C_1Pip][NTf_2]$, $[C_3C_1Py][NTf_2]$ and $[C_4C_1Py][NTf_2]$, respectively. The cationic volumes of the ILs estimated for the studied ILs are reported in Table 3 along with the anionic volume previously reported [18,39].

Table 4 presents the isobaric thermal expansion coefficients, α_p, of the studied ILs, which were calculated, at a fixed pressure, through the application of the Eq. (3)

$$\alpha_p = -\frac{1}{\rho}\left(\frac{\partial \rho}{\partial T}\right)_p = -\left(\frac{\partial \ln \rho}{\partial T}\right)_p \quad (3)$$

where ρ is the density in kg m^{-3}, T is the temperature in K. For the studied ILs, the α_p values range from 6.2×10^{-4} to 6.5×10^{-4} K^{-1}, which are in the same order of magnitude with those reported for other ILs families [13,18,21,22,48,55,56] and in good agreement with those reported in our previous work [30]. Nevertheless, the α_p values obtained are lower than the expansivities presented by organic solvents. The isobaric thermal expansion coefficients increase in the following IL cation sequence: $[C_3C_1Py]^+ > [C_4C_1Py]^+ > [C_4C_1Pip]^+ > [C_3C_1Pip]^+$ indicating that the increase of the alkyl chain size, of the pyridinium-based ILs, leads to a thermal expansion decrease, and, more interestingly, that the

Table 3
Ionic volumes, V, determined using Gardas and Coutinho Group Contribution Model [39] for the studied ILs.

Ionic species	V (Å^3)
Cation	
$[C_3C_1Pip]^+$	249
$[C_4C_1Pip]^+$	277
$[C_3C_1Py]^+$	230
$[C_4C_1Py]^+$	258
Anion[a]	
$[NTf_2]^-$	248

[a] Anion volume taken from previous works [18,39].

Table 4
Coefficients of thermal expansion, α_p, for studied ILs.

IL	10^4 ($\alpha_p \pm \sigma$)[a] (K^{-1})
$[C_3C_1Pip][NTf_2]$	6.21 ± 0.08
$[C_4C_1Pip][NTf_2]$	6.23 ± 0.08
$[C_3C_1Py][NTf_2]$	6.51 ± 0.09
$[C_4C_1Py][NTf_2]$	6.48 ± 0.09

[a] Expanded uncertainty with an approximately 95% level of confidence.

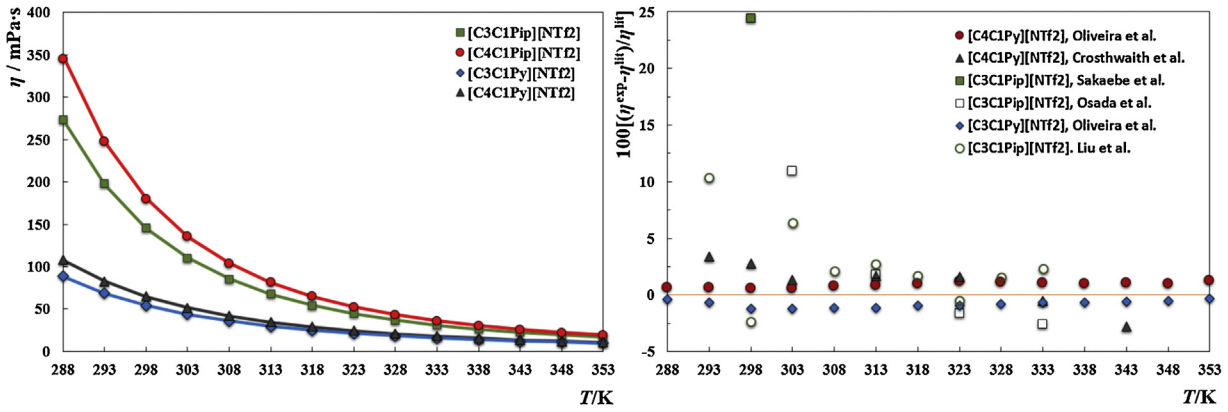

Fig. 2. Viscosity (left) and average relative deviations (right) between this work experimental data that available in the literature, as function of temperature [29,30,35,57,58]. The solid lines represent the Vogel-Fulcher-Tammann [38] group contribution correlation.

aromaticity of the pyridinium IL allows higher thermal expansivities.

3.2. Viscosity

The experimental dynamic viscosity data for the four ILs studied are presented in Table 2 and depicted in Fig. 2. The relative deviations between the data collected in this work and those reported in literature [29,30,35,57,58] are depicted in Fig. 2. Viscosity measurements are particularly affected by the presence of impurities (particularly water) and therefore larger deviations from the literature data are observed.

Small average absolute relative deviations of 0.79% and 0.91% for $[C_3C_1Py][NTf_2]$ and $[C_4C_1Py][NTf_2]$, respectively, were obtained towards viscosity data previously reported by us [30]. Nonetheless, higher deviations, 2.0, 3.3, 24.4 and 4.5%, were obtained against data for $[C_4C_1Py][NTf_2]$ from Crosthwaite et al. [58], and for $[C_3C_1Pip][NTf_2]$ from Liu et al. [35], Sakaebe et al. [57] and Osada et al. [29], respectively. The reasons for such a discrepancy must be related to the temperature control, presence of impurities and/or the measurement method used.

Viscosity is the internal resistance of a fluid to a shear stress, and in general, ILs present higher viscosities than those of conventional molecular solvents. The dynamic viscosities for the studied ILs decrease in the following IL cation sequence: $[C_4C_1Pip]^+ > [C_3C_1Pip]^+ > [C_4C_1Py]^+ > [C_3C_1Py]^+$, as presented in Fig. 2. Similar to the behavior observed for the densities if one takes into account also the results for an aromatic imidazolium, $[C_4C_1im][NTf_2]$ [59], and an non-aromatic pyrrolidinium, $[C_4C_1pyr][NTf_2]$ [60], the viscosities seem affected by the cation's aromaticity, with the non-aromatic compounds presenting higher viscosities than the aromatic ones: $[C_4C_1Pip]^+ > [C_4C_1Pyr]^+ > [C_4C_1Py]^+ > [C_4C_1im]^+$. The trend of the viscosity dependency on the cation's family and alkyl chain length are inverse to that observed for the density. If one pictures the IL's charged headgroups and anions playing the major role on the reasonably homogeneously distribution of the ILs [61], with the equilibrium average distance decided mainly by their short-range interactions, one easily portraits that the viscosity will be greatly affected by the cation's inherent interactions and ultimately their impact on the IL structure and bulk distribution. Although, the pyridinium π–π interactions could suggest higher resistance to shear stress due to a more rigid IL structure and bulk distribution, the results in Fig. 2 show the opposite, with lower viscosities for the pyridinium ILs. However, these results do not appear entirely as a surprise since the π–π interactions will also lend a more rigid ring structure and induce a more organized bulk distribution in comparison with the more flexible piperidinium ring that leads to a less rigid IL structure and to a more entanglement of the rings in the liquid phase. This effect, observed also in common organic solvents like the case of benzene and cyclohexane, denotes the entropic effects overpowering the enthalpic and controlling the resistance of the IL to a shear stress.

The description of viscosities for the ILs studied was carried out using the group contribution method, based on the Vogel-Fulcher-Tammann,

$$\ln \eta = A_\eta + \frac{B_\eta}{(T - T_{0\eta})} \tag{4}$$

where η is the dynamic viscosity in mPa s; T is the temperature in K; and A_η, B_η, and $T_{0\eta}$ are adjustable parameters. The parameters A_η, B_η, and $T_{0\eta}$ were estimating by correlating the experimental data and are presented in Table 5. The fitting results are depicted in Fig. 2 and present an average absolute relative deviations of 0.11% for $[C_3C_1Pip][NTf_2]$, 0.13% for $[C_4C_1Pip][NTf_2]$, 0.027% for $[C_3C_1Py][NTf_2]$ and 0.087% for $[C_4C_1Py][NTf_2]$.

3.3. Refractive index

Experimental refractive index for the studied compounds are presented in Table 2 and depicted in Fig. 3 and cover the temperature range 288.15–353.15 K, in steps of 5 K. The temperature interval was scanned upward and downward and no temperature hysteresis effects were observed. To the best of our knowledge, refractive index data for the studied ILs are here reported for the first time. The refractive index values for the $[NTf_2]$ anion-based ILs decrease in the follow cationic sequence: $[C_4C_1Py]^+ > [C_3C_1Py]^+ > [C_4C_1Pip]^+ > [C_3C_1Pip]^+$.

The refractive index for the ILs studied were also fitted with the group contribution method proposed by Gardas and Coutinho [38], which are depicted in Fig. 3, and that follows a linear function of the form,

$$n_D = A_{n_D} - B_{n_D} T \tag{5}$$

Table 5
Vogel-Fulcher-Tammann correlation parameters, A_η, B_η and $T_{0\eta}$, for the viscosity of the studied ILs.

IL	A_n	B_n (K)	$T_{0\eta}$ (K)
$[C_3C_1Pip][NTf_2]$	−1.64	759	184
$[C_4C_1Pip][NTf_2]$	−1.79	811	182
$[C_3C_1Py][NTf_2]$	−1.58	689	175
$[C_4C_1Py][NTf_2]$	−1.84	774	170

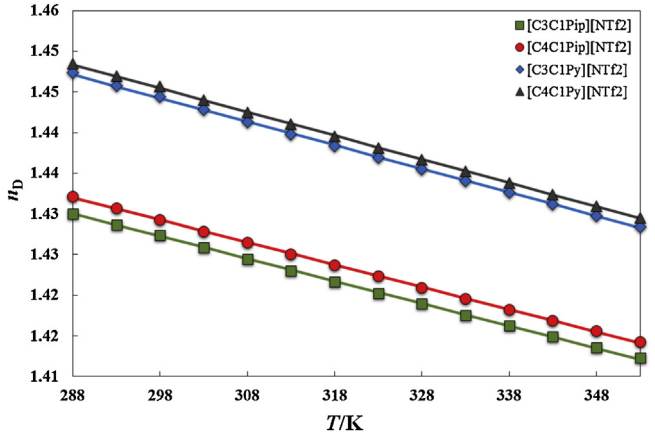

Fig. 3. Refractive index as function of temperature. The solid lines represent the Gardas and Coutinho [38] group contribution correlation.

$$A_{n_D} = \sum_{i=1}^{k} n_i a_{i,n_D} \tag{6}$$

$$B_{n_D} = \sum_{i=1}^{k} n_i b_{i,n_D} \tag{7}$$

where n_i is the number of groups of type i and k is the total number of different groups in the molecule. The estimated parameters a_{i,n_D} and b_{i,n_D} for the studied ILs and are given in Table 6. The average absolute relative deviation between the experimental and the fitting are 0.0047% for $[C_3C_1Pip][NTf_2]$, 0.0042% for $[C_4C_1Pip][NTf_2]$, 0.0049% for $[C_3C_1Py][NTf_2]$ and 0.0045% for $[C_4C_1Py][NTf_2]$.

The derived molar refractions, R_m, free volumes, f_m, and polarizabilities were additionally determined as follows [62–64]:

$$\frac{\alpha_0}{4\pi\varepsilon_0} = \left(\frac{n_D^2 - 1}{n_D^2 + 2}\right)\frac{3M}{4\pi\rho N_A} \tag{8}$$

where α_0 is the electronic polarizability, ε_0 the vacuum permittivity, ρ the compound's density, M the molecular weight and N_A the Avogadro number

$$R_m = \frac{N_A\alpha_0}{3\varepsilon_0} = \frac{n_D^2 - 1}{n_D^2 + 2}V_m \tag{9}$$

$$f_m = V_m - R_m \tag{10}$$

Similar to the viscosity the refractive indices are independent of the IL molecular weight and molar volumes but dependent on the cationic structure, with the pyridinium ILs presenting higher refractive indices than the piperidinium. Nonetheless, the piperidinium free volumes and molar refractions are higher than those of the homologous pyridinium, the values of which are summarized in Table 7, denoting once more the effect of the aromaticity of the pyridinium on the IL structure and on the polarizability.

Table 6
Group contribution parameters, a_{i,n_D} and b_{i,n_D}, determined using Gardas and Coutinho group contribution method for the refractive index [38].

Ionic species	a_{i,n_D}	b_{i,n_D} ($\times 10^{-4}$ K^{-1})
Cation		
$[C_3C_1Pip]^+$	1.4468	2.009
$[C_4C_1Pip]^+$	1.4487	2.006
$[C_3C_1Py]^+$	1.4679	2.148
$[C_4C_1Py]^+$	1.4679	2.160
Anion		
$[NTf_2]^-$ [38]	0.0628	0.7506

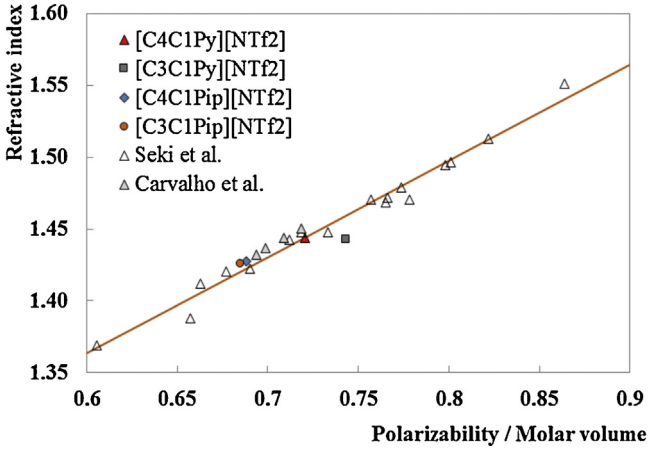

Fig. 4. Relationship between refractive index and polarizability/molecular volume for ILs at 303.15 K. The white triangles and the solid line represent the experimental data and correlation of Seki et al. [65], respectively. The grey triangles represent the experimental data reported in a previous work [66].

Recently, on the premise that refractive indices are an indication of the dielectric response to an electrical field, induced by electromagnetic waves, and that refractive indices can be considered as the first order approximation response to electronic polarization within an instantaneous time scale, Seki et al. [65] evaluated the refractive indices of 17 ILs, as function of temperature, against theoretical polarizabilities obtained through *ab initio* calculations, and proposed a correlation between the refractive index and the polarizability normalized in terms of the molecular volume. Following the work of Seki et al. [65] we have extended the correlation to the studied ILs, as done previously [66] for several ammonium and phosphonium ILs, showing that the correlation is able to predict the refractive index from polarizability and vice versa, within the uncertainty of the correlation, as depicted in Fig. 4.

3.4. Surface tension

The surface tension values for the $[NTf_2]$ anion-based ILs are presented in Table 8 and plotted in Fig. 5. Surface tension for the $[C_3C_1Pip][NTf_2]$ and $[C_3C_1Py][NTf_2]$ has already been reported in literature [29,67,68]. Using dynamic light scattering, Osada et al. [29] reported surface tension data for $[C_3C_1Pip][NTf_2]$ that presents average absolute relative deviations of 1.34%, while deviations of 0.48% were found against a 298 K surface tension point measured by us [67], on a previous work and using the same equipment. Furthermore, average absolute relative deviations of 3.24% were obtained against $[C_3C_1Py][NTf_2]$ data determined using the Du Noüy ring method, previously reported by us [68]. The deviations found seem related to the trace amounts of water, the technique employed and/or the sample purity.

The experimental surface tension values show that the IL cation plays a significant role in the structural organization of the IL at the air–liquid interface. The pyridinium and piperidinium-based ILs, investigated, follow the same trend as observed for

Table 7
Refractive indices, isotropic polarizabilities, derived molar refractions, R_m, and free volumes, f_m, at 298.15 K.

IL	n_D	Polarizability (bohr^3)	R_m (cm^3 mol^{-1})	f_m (cm^3 mol^{-1})
$[C_3C_1Pip][NTf_2]$	1.42739	205.73	76.90	222.38
$[C_4C_1Pip][NTf_2]$	1.42928	218.11	81.53	234.55
$[C_3C_1Py][NTf_2]$	1.44440	214.24	76.40	210.98
$[C_4C_1Py][NTf_2]$	1.44566	219.91	81.06	223.12

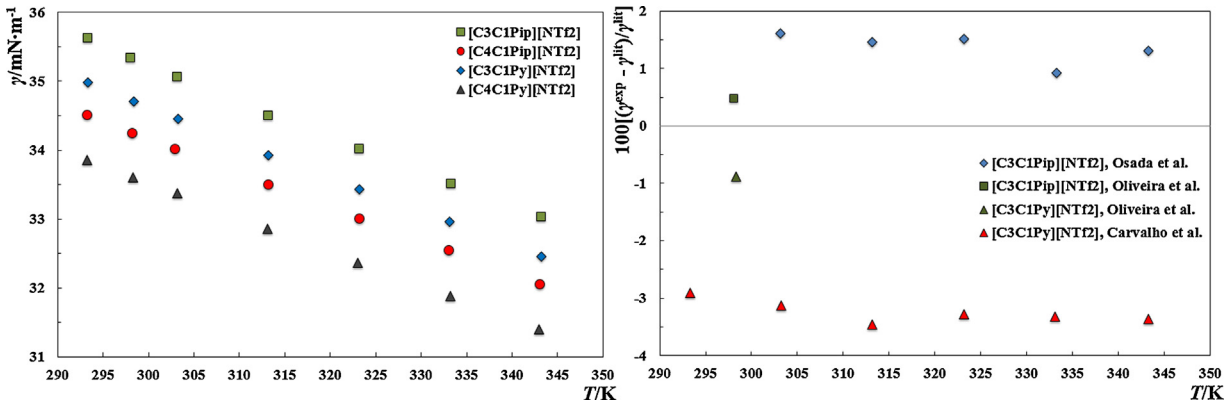

Fig. 5. Surface tension (left) and average relative deviations (right) as function of temperature for the studied ILs.

other ILs, with the increase of the alkyl chain length leading to a decrease of the surface tension. Furthermore, both pyridinium- and piperidinium-based ILs present higher surface tensions than those reported for the corresponding imidazolium-based ILs, indicating stronger intermolecular interactions and thus, an air–liquid interface arrangement with higher surface energies. This trend is in agreement with previous surface tension data for other imidazolium- [29,69,70], pyrrolidinium- [68,70] and pyridinium-based [70] ILs. It is well established that the surface tension is intrinsically related with the part of the molecule that is present at the interface and in the case of ILs the cation has a important role. Therefore, having the smaller cation alkyl chain sized ILs presenting higher surface tension comes straightforward. Nonetheless, surface tension data shows that the piperidinium less rigid ring allows a better surface arrangement, of the molecules, than the more rigid aromatic ring of the pyridinium cation.

3.4.1. Surface thermodynamic properties

The surface thermodynamic properties, namely, the surface entropy and the surface enthalpy, were derived using the quasi-linear dependence of the surface tension with temperature. The surface entropy, S^{γ}, can be calculated according to the following equation [71,72]

$$S^{\gamma} = -\left(\frac{d\gamma}{dT}\right) \tag{11}$$

while the surface enthalpy, H^{γ}, according to [71,72]

$$H^{\gamma} = \gamma - T\left(\frac{d\gamma}{dT}\right) \tag{12}$$

The values of the thermodynamic functions for the ILs studied and the respective expanded uncertainties [73] are presented in Table 9. The surface entropy decreases with the increase of the alkyl chain following the decrease of the surface tension. Even though the estimation of the entropies and enthalpies have some uncertainties associated they indicate that either the increase of the cation alkyl chain, from a propyl to a butyl, or the aromaticity of the cation's ring promotes a significant change on the order of the surface. Nonetheless, the low surface entropies obtained are an indication of a high surface organization as well as a highly structured liquid phase.

3.4.2. Estimated critical temperatures

The critical temperature of fluids is one of the most important thermophysical properties, commonly used in corresponding state correlations involving equilibrium and transport properties of fluids [74]. Nonetheless, the direct determination of the critical temperatures of ILs would be an arduous task due to IL intrinsic nature with negligible vapor pressures and relatively low decomposition temperatures. Nonetheless, the critical temperature can

Table 8
Surface tension, γ, for the studied ILs as function of temperature and at atmospheric pressure.

$[C_3C_1Pip][NTf_2]$		$[C_4C_1Pip][NTf_2]$		$[C_3C_1Py][NTf_2]$		$[C_4C_1Py][NTf_2]$	
T (K)	γ (mN m^{-1})	T (K)	γ (mN m^{-1})	T (K)	γ (mN m^{-1})	T (K)	γ (mN m^{-1})
293.4	35.6	293.3	34.5	293.3	35.0	293.3	33.9
298.0	35.3	298.2	34.2	298.3	34.7	298.3	33.6
303.1	35.1	302.9	34.0	303.3	34.5	303.2	33.4
313.2	34.5	313.2	33.5	313.2	33.9	313.1	32.9
323.2	34.0	323.2	33.0	323.2	33.4	323.0	32.4
333.3	33.5	333.0	32.5	333.1	33.0	333.2	31.9
343.3	33.0	343.1	32.1	343.2	32.5	343.0	31.4

[a] Standard temperature uncertainty is $u(T) = \pm 0.1$ K, and the surface tension expanded uncertainty is $U_c(\gamma) = 0.1$ mN m^{-1}, with an approximately 95% level of confidence.

Table 9
Surface thermodynamic functions of the studied ILs and estimated critical temperatures, using both Eötvös (Eot) [75] and Guggenheim (Gug) [76] empirical equations.

IL	$(S^{\gamma} \pm \sigma)$[a] ($\times 10^{-5}$ J m^{-2} K^{-1})	$(H^{\gamma} \pm \sigma)$[a] ($\times 10^{-2}$ J m^{-2})	$(T_c)_{Eot}$ (K)	$(T_c)_{Gug}$ (K)
$[C_3C_1Pip][NTf_2]$	5.18 ± 0.08	5.08 ± 0.03	1229 ± 16	1127 ± 12
$[C_4C_1Pip][NTf_2]$	4.92 ± 0.03	4.89 ± 0.01	1259 ± 5	1144 ± 4
$[C_3C_1Py][NTf_2]$	5.05 ± 0.05	4.98 ± 0.02	1259 ± 8	1134 ± 7
$[C_4C_1Py][NTf_2]$	4.95 ± 0.03	4.84 ± 0.01	1242 ± 4	1124 ± 3

[a] Expanded uncertainty with an approximately 95% level of confidence.

be estimated by means of the Eötvös [75] and Guggenheim [76] equations as follows,

$$\gamma\left(\frac{M}{\rho}\right)^{2/3} = K(T_c - T) \quad (13)$$

$$\gamma = K\left(1 - \frac{T}{T_c}\right)^{11/9} \quad (14)$$

where T_c is the critical temperature and K is a fitted parameter. Both equations reflect the fact that the surface tension becomes null at the critical point and although an overestimation of the critical temperature is expected, since at the critical point the pressure becomes the critical pressure, these equations provide reasonable estimations [74,77]. The critical temperature values, Table 9, estimated from the surface tension data follow the same trend of the surface tension, showing the aromaticity effect of the cation's ring, with critical temperatures similar to other ILs.

4. Conclusions

Experimental data on density, viscosity, refractive index and surface tension data of four ILs (two piperidinium and two pyridinium) with the bis(trifluoromethylsulfonyl)imide anion were measured in the temperature range between 288.15 and 353.15 K and at atmospheric pressure. All the properties investigated show an effect both from the cation's alkyl chain size increase and from the aromaticity of the cation's ring. Even though one could foresee the pyridinium π–π interactions leading to a more rigid, compact and organized bulk distribution and thus to higher density values, it also has an important impact on surface and dynamic properties, like surface tensions and viscosities. The less rigid structure of the piperidinium promotes more entanglement in the bulk liquid phase and consequently higher resistance to shear stress (higher viscosities) and better surface arrangement (higher surface tensions). This effect of the aromaticity, already reported for common organic solvents like the case of benzene and cyclohexane, denotes the entropic effects overpowering the enthalpic.

The group contribution methods proposed by Gardas and Coutinho for density, viscosity and refractive index were evaluated and fitted to the experimental data, allowing thus, to propose new parameters for the cations investigated.

Acknowledgements

The authors acknowledge FEDER funds through the COMPETE operational program and Fundação para a Ciência e Tecnologia – FCT through the project CICECO - FCOMP-01-0124-FEDER-037271 (Ref. FCT PEst-C/CTM/LA0011/2013) and P.J.C. and A.B. postdoctoral grants SFRH/BPD/82264/2011 and SFRH/BPD/77858/2011, respectively.

References

[1] M.J. Earle, J.M.S.S. Esperanca, M.A. Gilea, J.N. Canongia Lopes, L.P.N. Rebelo, J.W. Magee, K.R. Seddon, J.A. Widegren, Nature 439 (2006) 831–834.
[2] K.J. Baranyai, G.B. Deacon, D.R. MacFarlane, J.M. Pringle, J.L. Scott, Aust. J. Chem. 57 (2004) 145–147.
[3] M. Smiglak, W.M. Reichert, J.D. Holbrey, J.S. Wilkes, L. Sun, J.S. Thrasher, K. Kirichenko, S. Singh, A.R. Katritzky, R.D. Rogers, Chem. Commun. (2006) 2554–2556.
[4] A.B. Pereiro, H. Veiga, J.M.S.S. Esperança, A. Rodríguez, J. Chem. Thermodyn. 41 (2009) 1419–1423.
[5] P. Wasserscheid, T. Welton, Ionic Liquids in Synthesis, Wiley-VCH, Weinheim, Germany, 2008.
[6] N.V. Plechkova, K.R. Seddon, Chem. Soc. Rev. 37 (2008) 123–150.
[7] L.P.N. Rebelo, J.N.C. Lopes, J.M.S.S. Esperança, H.J.R. Guedes, J. Łachwa, V. Najdanovic-Visak, Z.P. Visak, Acc. Chem. Res. 40 (2007) 1114–1121.
[8] D.R. MacFarlane, K.R. Seddon, Aust. J. Chem. 60 (2007) 3–5.
[9] R.D. Rogers, K.R. Seddon, Sci. 302 (2003) 792–793.
[10] K.R. Seddon, J. Chem. Technol. Biotechnol. 68 (1997) 351–356.
[11] M.A.A. Rocha, F.M.S. Ribeiro, A.I.M.C.L. Ferreira, J.A.P. Coutinho, L.M.N.B.F. Santos, J. Mol. Liq. 188 (2013) 196–202.
[12] A.A.M. Beigi, M. Abdouss, M. Yousefi, S.M. Pourmortazavi, A. Vahid, J. Mol. Liq. 177 (2013) 361–368.
[13] C.M.S.S. Neves, K.A. Kurnia, J.A.P. Coutinho, I.M. Marrucho, J.N.C. Lopes, M.G. Freire, L.P.N. Rebelo, J. Phys. Chem. B 117 (2013) 10271–10283.
[14] P.J. Carvalho, T. Regueira, L.M.N.B.F. Santos, J. Fernandez, J.A.P. Coutinho, J. Chem. Eng. Data 55 (2010) 645–652.
[15] M.G. Freire, A.R.R. Teles, M.A.A. Rocha, C.M.S.S. Neves, P.J. Carvalho, D.V. Evtuguin, L.M.N.B.F. Santos, J.A.P. Coutinho, B. Schröder, J. Chem. Eng. Data 56 (2011) 4813–4822.
[16] R. Gomes de. Azevedo, J.M.S.S. Esperança, V. Najdanovic-Visak, Z.P. Visak, H.J.R. Guedes, M. Nunes da Ponte, L.P.N. Rebelo, J. Chem. Eng. Data 50 (2005) 997–1008.
[17] J.M.S.S. Esperança, Z.P. Visak, N.V. Plechkova, K.R. Seddon, H.J.R. Guedes, L.P.N. Rebelo, J. Chem. Eng. Data 51 (2006) 2009–2015.
[18] R.L. Gardas, H.F. Costa, M.G. Freire, P.J. Carvalho, I.M. Marrucho, I.M.A. Fonseca, A.G.M. Ferreira, J.A.P. Coutinho, J. Chem. Eng. Data 53 (2008) 805–811.
[19] R.L. Gardas, M.G. Freire, P.J. Carvalho, I.M. Marrucho, I.M.A. Fonseca, A.G.M. Ferreira, J.A.P. Coutinho, J. Chem. Eng. Data 52 (2007) 80–88.
[20] M. Tariq, A.P. Serro, J.L. Mata, B. Saramago, J.M.S.S. Esperança, J.N.C. Lopes, L.P.N. Rebelo, Fluid Phase Equilib. 294 (2010) 131–138.
[21] M. Tariq, P.A.S. Forte, M.F.C. Gomes, J.N.C. Lopes, L.P.N. Rebelo, J. Chem. Thermodyn. 41 (2009) 790–798.
[22] J. Jacquemin, P. Husson, V. Majer, A.A.H. Padua, M.F.C. Gomes, Green Chem. 10 (2008) 944–950.
[23] M. García-Mardones, I. Bandrés, M.C. López, I. Gascón, C. Lafuente, J. Solution Chem. 41 (2012) 1836–1852.
[24] N.M. Yunus, M.I. Abdul Mutalib, Z. Man, M.A. Bustam, T. Murugesan, J. Chem. Thermodyn. 42 (2010) 491–495.
[25] I. Bandrés, B. Giner, H. Artigas, C. Lafuente, F.M. Royo, J. Chem. Eng. Data 54 (2009) 236–240.
[26] I. Bandrés, B. Giner, I. Gascon, M. Castro, C. Lafuente, I. Gascón, I. Bandrés, I. Gasco′n, J. Phys. Chem. B 112 (2008) 12461–12467.
[27] B. Mokhtarani, A. Sharifi, H.R. Mortaheb, M. Mirzaei, M. Mafi, F. Sadeghian, J. Chem. Thermodyn. 41 (2009) 323–329.
[28] L. Gala, J. Ribe, F. Onink, G.W. Meindersma, L.G. Sánchez, J.R. Espel, A.B. de Haan, B. De Haan, J. Chem. Eng. Data 54 (2009) 2803–2812.
[29] R. Osada, T. Hoshino, K. Okada, Y. Ohmasa, M. Yao, J. Chem. Phys. 130 (2009) 184705.
[30] F.S. Oliveira, M.G. Freire, P.J. Carvalho, J.A.P. Coutinho, J.N.C. Lopes, L.P.N. Rebelo, I.M. Marrucho, J. Chem. Eng. Data 55 (2010) 4514–4520.
[31] E. Gómez, N. Calvar, Á. Domínguez, E.A. Macedo, J. Chem. Thermodyn. 42 (2010) 1324–1329.
[32] N. Papaiconomou, O. Zech, P. Bauduin, J.M. Lévêque, W. Kunz, Electrochim. Acta 70 (2012) 124–130.
[33] P. Verdía, M. Hernaiz, E.J. González, E.A. Macedo, J. Salgado, E. Tojo, J. Chem. Thermodyn. 69 (2014) 19–26.
[34] H. Sakaebe, H. Matsumoto, K. Tatsumi, J. Power Sources 146 (2005) 693–697.
[35] K. Liu, Y.X. Zhou, H.B. Han, S.S. Zhou, W.F. Feng, J. Nie, H. Li, X.J. Huang, M. Armand, Z.B. Zhou, Electrochim. Acta 55 (2010) 7145–7151.
[36] M.G. Freire, C.M.S.S. Neves, I.M. Marrucho, J.A.P. Coutinho, A.M. Fernandes, J. Phys. Chem. A 114 (2010) 3744–3749.
[37] M.G. Freire, P.J. Carvalho, R.L. Gardas, I.M. Marrucho, L.M.N.B.F. Santos, J.A.P. Coutinho, J. Phys. Chem. B 112 (2008) 1604–1610.
[38] R.L. Gardas, J.A.P. Coutinho, AIChE J. 55 (2009) 1274–1290.
[39] R.L. Gardas, J.A.P. Coutinho, Fluid Phase Equilib. 263 (2008) 26–32.
[40] E.P. Grishina, L.M. Ramenskaya, M.S. Gruzdev, O.V. Kraeva, J. Mol. Liq. 177 (2013) 267–272.
[41] G.C. Tian, H.K. Feng, J.L. Zhang, Adv. Mater. Res. 549 (2012) 152–156.
[42] C.M.S.S. Neves, M.L.S. Batista, A.F.M. Cláudio, L.M.N.B.F. Santos, I.M. Marrucho, M.G. Freire, J.A.P. Coutinho, J. Chem. Eng. Data 55 (2010) 5065–5073.
[43] H.F.D. Almeida, H. Passos, J.A. Lopes-da-Silva, A.M. Fernandes, M.G. Freire, J.A.P. Coutinho, J. Chem. Eng. Data 57 (2012) 3005–3013.
[44] H.F.D. Almeida, A.R.R. Teles, J.A. Lopes-da-Silva, M.G. Freire, J.A.P. Coutinho, J. Chem. Thermodyn. 54 (2012) 49–54.
[45] R.L. Gardas, M.G. Freire, P.J. Carvalho, I.M. Marrucho, I.M.A. Fonseca, A.G.M. Ferreira, J.A.P. Coutinho, J. Chem. Eng. Data 52 (2007) 1881–1888.
[46] M. Blesic, M. Swadzba-Kwasny, T. Belhocine, H.Q.N. Gunaratne, J.N.C. Lopes, M.F.C. Gomes, A.A.H. Padua, K.R. Seddon, L.P.N. Rebelo, Phys. Chem. Chem. Phys. 11 (2009) 8939–8948.
[47] K. Machanová, A. Boisset, Z. Sedláková, M. Anouti, M. Bendová, J. Jacquemin, J. Chem. Eng. Data 57 (2012) 2227–2235.
[48] P. Kilaru, G.A. Baker, P. Scovazzo, J. Chem. Eng. Data 52 (2007) 2306–2314.
[49] a.d.o.U.o.K.a.F.K.G. TURBOMOLE V6.1 2009, 1989-2007, 25 GmbH, since 2007; available from http://www.turbomole.com
[50] A.K.F. Eckert, COSMOtherm Version C2.1 Release 01.08, COSMOlogic GmbH & Co. KG, Leverkusen, Germany, 2006.
[51] R. Gomes de. Azevedo, J.M.S.S. Esperanca, J. Szydlowski, Z.P. Visak, P.F. Pires, H.J.R. Guedes, L.P.N. Rebelo, J. Chem. Thermodyn. 37 (2005) 888–899.
[52] J.M.S.S. Esperança, H.J.R. Guedes, M. Blesic, L.P.N. Rebelo, J. Chem. Eng. Data 51 (2006) 237–242.
[53] K. Paduszyński, J. Chiyen, D. Ramjugernath, T.M. Letcher, U. Domańska, Fluid Phase Equilib. 305 (2011) 43–52.
[54] C. Ye, J.M. Shreeve, J. Phys. Chem. A 111 (2007) 1456–1461.

[55] J. Jacquemin, P. Husson, V. Mayer, I. Cibulka, J. Chem. Eng. Data 52 (2007) 2204–2211.
[56] Z. Gu, J.F. Brennecke, J. Chem. Eng. Data 47 (2002) 339–345.
[57] H. Sakaebe, H. Matsumoto, Electrochem. Commun. 5 (2003) 594–598.
[58] J.M. Crosthwaite, M.J. Muldoon, J.K. Dixon, J.L. Anderson, J.F. Brennecke, J. Chem. Thermodyn. 37 (2005) 559–568.
[59] K.R. Harris, M. Kanakubo, L.A. Woolf, J. Chem. Eng. Data 51 (2006) 1161–1167.
[60] F.M. Gaciño, T. Regueira, L. Lugo, M.J.P. Comuñas, J. Fernández, J. Chem. Eng. Data 56 (2011) 4984–4999.
[61] Y. Wang, G.A. Voth, J. Am. Chem. Soc. 127 (2005) 12192–12193.
[62] J.N. Israelachvili, Intermolecular and Surface Forces, Academic Press, San Diego, 2011.
[63] A.R.H. Goodwin, K.N. Marsh, W.A. Wakeham, Measurement of the Thermodynamic Properties of Single Phases, IUPAC Experimental Thermodynamics, vol. VI, Elsevier, Amsterdam, 2003.
[64] P. Brocos, A. Pineiro, R. Bravo, A. Amigo, Phys. Chem. Chem. Phys. 5 (2003) 550–557.
[65] S. Seki, S. Tsuzuki, K. Hayamizu, Y. Umebayashi, N. Serizawa, K. Takei, H. Miyashiro, J. Chem. Eng. Data 57 (2012) 2211–2216.
[66] P.J. Carvalho, S.P.M. Ventura, M.L.S. Batista, B. Schröder, F. Gonçalves, J. Esperança, F. Mutelet, J.A.P. Coutinho, J. Chem. Phys. 140 (2014) 064505.
[67] M.B. Oliveira, M. Domínguez-Pérez, O. Cabeza, J.A. Lopes-da-Silva, M.G. Freire, J.A.P. Coutinho, J. Chem. Thermodyn. 64 (2013) 22–27.
[68] P.J. Carvalho, C.M.S.S. Neves, J.A.P. Coutinho, J. Chem. Eng. Data 55 (2010) 3807–3812.
[69] P.J. Carvalho, M.G. Freire, I.M. Marrucho, A.J. Queimada, J.A.P. Coutinho, J. Chem. Eng. Data 53 (2008) 1346–1350.
[70] L.G. Sánchez, J.R. Espel, F. Onink, G.W. Meindersma, A.B. de Haan, J. Chem. Eng. Data 54 (2009) 2803–2812.
[71] A.W. Adamson, A.P. Gast, Physical Chemistry of Surfaces, John Wiley, New York, 1997.
[72] A.D. McNaught, A. Wikinson, Compendium of Chemical Therminology, IUPAC, Recommendations, Blackwell Science, Cambridge, U.K., 1997.
[73] J.C. Miller, J.N. Miller, Statistics for Analytical Chemistry, PTR Prentice Hall, Chichester, NY, 1993.
[74] B.E. Poling, J.M. Prausnitz, J.P. O'Connell, The Properties of Gases and Liquids, McGraw-Hill, New York, 2001.
[75] J.L. Shereshefsky, J. Phys. Chem. 35 (1930) 1712–1720.
[76] E.A. Guggenheim, J. Chem. Phys. 13 (1945) 253–261.
[77] K.S. Birdi, Handbook of Surface and Colloid Chemistry, CRC Press, Boca Raton, FL, 1997.